

Lesion evidence for the critical role of the intraparietal sulcus in spatial attention

Céline R. Gillebert¹, Dante Mantini², Vincent Thijs^{3,4}, Stefan Sunaert⁵, Patrick Dupont¹, Rik Vandenberghe^{1,4}

¹Laboratory for Cognitive Neurology, K.U.Leuven; ²Laboratory for Neuro- and Psychophysiology, K.U.Leuven;

³Vesalius Research Centre, Vlaams Instituut voor Biotechnologie; ⁴Neurology Department, University Hospitals Leuven; ⁵Radiology Department, University Hospitals Leuven; Herestraat 49, 3000 Leuven, Belgium

Running title: Orienting deficits after IPS lesions *Correspondence to:* Rik Vandenberghe. Neurology Department, University Hospitals Leuven, Herestraat 49 - bus 7003, B-3000 Leuven, Belgium. Tel: +3216344280, Fax: +3216344285. E-mail: rik.vandenberghe@uz.kuleuven.ac.be.

This is a pre-copy-editing, author-produced PDF of an article accepted for publication in Brain following peer review. The definitive publisher-authenticated version (Gillebert, C.R., Mantini, D., Thijs, V., Sunaert, S., Dupont, P., and Vandenberghe, R. (2011). Lesion evidence for the critical role of the intraparietal sulcus in spatial attention. Brain, 134:1694-1709.) is available online at: <http://dx.doi.org/10.1093/brain/awr085>.

Abstract

Based on lesion mapping studies, the inferior parietal lobule and temporoparietal junction are considered the critical parietal regions for spatial-attentional deficits. Lesion evidence for a key role of the intraparietal sulcus, a region featuring prominently in nonhuman primate studies and human functional imaging studies of the intact brain, is still lacking, probably due to the exceptional nature of isolated intraparietal sulcus lesions. We combined behavioral testing and functional imaging in 2 patients with a focal intraparietal sulcus lesion sparing the inferior parietal lobule and temporoparietal junction to examine the critical contribution of the intraparietal sulcus to spatial attention. HH had a focal ischemic lesion (1.8 cm^3) that was confined to the posterior segment of the left intraparietal sulcus, whereas NV had a partially reversible lesion of the middle segment of the right intraparietal sulcus extending into the superior parietal lobule (13.8 cm^3). The performance of these cases was contrasted with 5 cases with a classical inferior parietal lesion, as well as with a group of 31 age-matched controls. In the behavioral study the patients performed an orientation discrimination task on a peripheral target (eccentricity 7.6°) that was preceded by a central spatial cue. We manipulated both the cue validity (17% trials with an invalid spatial cue) and the presence of a competing distracter in the visual field contralateral to the target (17% double stimulation trials). The ability of the intraparietal sulcus patients to re-orient their spatial focus of attention and to select between competing stimuli was impaired for contralesional targets compared to controls, similarly to what we saw in the inferior parietal group. Furthermore, we could observe that the deficit in NV resolved with regression of the lesion. To further evaluate the correspondence between spatial-attentional deficits and the intraparietal sulcus lesions, we ascertained the functional integrity of the inferior parietal lobule and temporoparietal junction in HH using an event-related fMRI with the same task as in the behavioral study. His intraparietal sulcus lesion did not affect the task-related activation of the inferior parietal lobule or temporoparietal junction. Additionally, a resting-state fMRI study in HH and 62 controls revealed that his lesion did not affect the topology of the ventral attention network nor the strength of its main inter- and intrahemispheric connections. Our findings demonstrate that the human superior parietal cortex critically contributes to spatially selective attention.

Key Words: spatial attention; parietal cortex; stroke; neuroimaging

Abbreviations: IPS = intraparietal sulcus; IPL = inferior parietal lobule; TPJ = temporopari-

etal junction; SPL = superior parietal lobule; STG = superior temporal gyrus; IFG = inferior frontal gyrus; RSN = resting-state network; MRI = magnetic resonance imaging; FLAIR = fluid attenuated inversion recovery; VLSM = voxel-based lesion-symptom mapping; IC = independent component

Introduction

Decades of clinical neurology have highlighted the critical role of parietal cortex in spatially selective attention (Critchley, 1953; Mesulam, 1990, 2000; Corbetta et al., 2008; Riddoch et al., 2010). Neuroanatomically more refined techniques in healthy human subjects have implicated separate parts (Husain and Nachev, 2007) of parietal cortex, such as the intraparietal sulcus (IPS) (Corbetta and Shulman, 2002; Hung et al., 2005; Molenberghs et al., 2007, 2008; Vandenberghe and Gillebert, 2009), the temporoparietal junction (TPJ) (Corbetta et al., 2000; Downar et al., 2000; Corbetta and Shulman, 2002; Vossel et al., 2009) or the superior parietal lobule (SPL) (Vandenberghe et al., 2001; Yantis et al., 2002) in different attentional processes, including, among others, endogenous control (Corbetta and Shulman, 2002), spatial reorienting (Corbetta et al., 2008) and shifting (Vandenberghe et al., 2001; Yantis et al., 2002), the computation of a saliency map (Molenberghs et al., 2008) or the detection of low-frequency events (Downar et al., 2000; Vossel et al., 2009). The IPS itself is composed of functionally specialised areas in humans and in nonhuman primates (Gottlieb et al., 1998). The horizontal segment of the IPS contains the putative human homologue of monkey area LIP, where neurons are strongly modulated by spatial attention and code for a topographical representation of attentional weights (Gottlieb et al., 1998; Sereno et al., 2001; Bundesen et al., 2005; Molenberghs et al., 2008). More posteriorly, the human IPS contains a series of visually responsive areas (denominated as IPS0/V7, IPS1, IPS2) with retinotopic representations of the contralateral visual field (Silver et al., 2005; Swisher et al., 2007; Wandell et al., 2007; Silver and Kastner, 2009; Sheremata et al., 2010) which are sensitive to the direction of attention (Yantis et al., 2002; Vandenberghe et al., 2005; Vandenberghe and Gillebert, 2009; Silver and Kastner, 2009; Bressler and Silver, 2010). To the left, the directional effect in IPS0 persists during short-term memory tasks in particular when set size is high (Sheremata et al., 2010). The exact monkey homologue of these posterior IPS regions is still under debate (Tootell et al., 1998; Koyama et al., 2004; Orban et al., 2006) and to the best of our knowledge isolated lesions in humans have not been reported previously. The key role of IPS in selective attention is supported by transcranial

magnetic stimulation studies showing that disruption of the posterior parietal cortex activity can induce attentional deficits in healthy subjects, including a failure to detect (Pascual-Leone et al., 1994; Koch et al., 2005), identify (Hung et al., 2005) or visually track (Battelli et al., 2009) targets in the visual field contralateral to the stimulation site under conditions of bilateral simultaneous stimulation (see Driver et al., 2010; Sack, 2010, for reviews).

Lesion evidence that IPS is critically important for spatially selective attention in patients is lacking. A highly influential lesion study in parietal stroke patients attributed the spatial-attentional deficit, as measured in Posner’s invalidity paradigm (Posner et al., 1984), to inferior rather than superior parietal damage (Friedrich et al., 1998). Lesion overlap (Vallar and Perani, 1986; Karnath et al., 2001; Karnath et al., 2003; Bays et al., 2010), lesion subtraction (Mort et al., 2003; Grandjean et al., 2008; Ticini et al., 2010) and voxel-based lesion-symptom mapping (VLSM) (Karnath et al., 2004, 2010) studies in neglect and extinction have also emphasized the contribution of the inferior parietal lobule (IPL) (Vallar and Perani, 1986; Mort et al., 2003; Bays et al., 2010), TPJ (Karnath et al., 2003; Grandjean et al., 2008; Ticini et al., 2010) and posterior third of the superior temporal gyrus (STG) (Karnath et al., 2001, 2004, 2010) rather than IPS.

The typical parietal lesions causing neglect and extinction have their center of gravity in IPL (Mort et al., 2003) but often extend into the lateral bank of IPS (Molenberghs et al., 2008). In a recent model of visual attention that integrates evidence from multiple scientific disciplines, the occurrence of spatial neglect after acute stroke is attributed to the combined effect of a re-orienting problem originating from TPJ and a lateralized attentional bias originating from IPS (Corbetta and Shulman, 2002; Corbetta et al., 2005; Carter et al., 2010). This model is partly based on task-related (Corbetta et al., 2005) and resting-state (He et al., 2007; Carter et al., 2010) functional magnetic resonance imaging (fMRI) studies in patients with neglect during the acute phase and after recovery. These provide evidence for alterations at a distance of the structural lesion, in activity of individual nodes and in connectivity between nodes (Alstott et al., 2009), within but also between functional networks (Corbetta, 2010).

Cases with cortical lesions restricted to IPS and sparing IPL are extremely valuable to evaluate whether IPS in its own right critically contributes to spatially selective attention in the intact brain and whether lesions of IPS can independently cause spatial-attentional deficits. Such lesions, however, are exceptional given the distribution of vascular territories in the human brain. We report performance of a hybrid valid/invalid cueing (Posner et al., 1984; Friedrich et al., 1998) and stimulus competition paradigm (Molenberghs et al., 2008) in two cases with a

Table 1 – Patient characteristics. Values in **bold** indicate a pathological score on the test. Abbreviations: M = male; F = female; L = left; R = right; time = time-to-stroke onset; VF = visual field; LL = left lower quadrantanopia. Bisection = percentage deviation to the patients right (positive) or left (negative) hand side. Omissions = omissions on the star cancellation test in left and right hemispace.

case	age	sex	lesion side	time (days)	volume (cm ³)	VF defect	bisection (%)	omissions (L/R)
IPS cases:								
HH	52	M	L	199	1.8	-	-11%	0/0
NV	23	F	R	4	13.8	-	4%	2/0
IPL cases:								
AN	65	M	R	4	72.5	-	19%	6/2
CK	62	M	R	7	31.3	LL	-3%	0/0
MD	67	M	R	36	81.5	-	7%	2/0
RE	77	M	R	232	27.0	-	5%	0/0
PS	67	M	R	4	63.2	-	4%	0/0

focal IPS lesion. Given the evidence from task-related and resting-state fMRI studies in neglect (Corbetta et al., 2005; He et al., 2007; Carter et al., 2010; Corbetta, 2010), we took special care to ascertain not only the structural but also the functional integrity of IPL and TPJ. Five cases with a typical IPL lesion served as positive controls.

Methods

The study was approved by the Ethics Committee, University Hospitals Leuven. All participants provided written informed consent in accordance with the Declaration of Helsinki.

Participants

Patients with ischemic lesions restricted to parietal cortex on clinical fluid attenuated inversion recovery (FLAIR) or diffusion-weighted MRI were consecutively recruited via the acute stroke unit of the University Hospitals Leuven, Belgium, or on occasion of their first post-stroke visit to the outpatient clinic. Extension into the insula or the posterior temporal cortex was permitted based on the known distribution of the vascular territory of the posterior branches of the middle cerebral artery. Exclusion criteria were age above 85 years, pre-existing structural lesions or extensive periventricular or subcortical white matter hyperintensities on MRI, presence of hemianopia, insufficient balance to sit autonomously in front of a computer, and general inability to understand and perform a computerized perceptual discrimination task. Visual perimetry was formally tested in each patient in a computerized manner. We screened a consecutive series of 870 patients, 7 of whom fulfilled the inclusion criteria (Table 1).

Two of the participants, HH and NV, had an IPS lesion that strictly spared IPL (Fig. 1A-D). HH (strictly right-handed male, 52 years; Table 1) had a focal lesion (volume = 1.8 cm³) that was confined to the posterior segment of left IPS (Fig. 1A,B). The lesion consisted of 2 juxtaposed components at Montreal Neurological Institute (MNI) coordinates x=-19, y=-72, z=36 (1.1 cm³) and x=-15, y=-67, z=59 (0.7 cm³). NV (strictly right-handed female, 23 years) had a lesion of the horizontal segment of right IPS (volume = 13.8 cm³) extending into SPL. The center of gravity was located at x=19, y=-64, z=47. She also had a second smaller asymptomatic FLAIR hyperintense lesion in the left postcentral gyrus (Suppl. Fig. 1A). NV's symptoms were strictly lateralized to the left foot and leg (numbness and weakness) and she also reported having hit the door jamb with her left side on several occasions. She was tested 4 days after her stroke (Fig. 1C,D, Suppl. Fig. 1A) and 107 days later when her lesions had significantly diminished (1.2 cm³) to a small portion of SPL (Suppl. Fig. 1B). As the underlying cause, HH had an arterial ischemia and NV a venous infarction. The 5 remaining parietal lesion patients had a classical arterial ischemic lesion that was confined to right IPL extending into the posterior part of STG and the insula (center of gravity: x=55, y=-37, z=19; Fig. 1E,F). In one of the IPL cases (AN, Table 1) 3% of the lesion overlapped with NV's lesion.

All patients participated in a computerized behavioral experiment and underwent a structural MRI. The IPS cases also participated in a task-related and resting-state fMRI experiment. Because HH and NV differed in age (Table 1) we recruited both elderly and young controls. For the behavioral experiment, 17 healthy subjects above the age of 50 (8 women, age 52-73) served as controls for HH and the IPL group, and 14 healthy subjects below the age of 35 (10 women, age 19-31) served as controls for NV. Sixteen healthy subjects (8 women, age 20-26) participated as controls in the task-related fMRI experiment and 62 healthy subjects (25 women, age 20-72) in the resting-state fMRI experiment.

Behavioral experiment

Stimulus presentation and response registration were controlled by a PC running Presentation 11.3 (Neurobehavioral systems, Albany, CA). Participants were seated at 50 cm from a 19-inch cathode ray tube monitor (resolution 1024×768 pixels, refresh rate 75 Hz).

A trial started with a warning cue (duration 150 ms), followed by a central spatial arrow cue pointing leftward or rightward (200 ms), a delay phase (200 ms) during which only the fixation dot (size 0.45°) was shown, and a test phase during which a peripheral grating was added (200 ms, size 3.5°, 0.5 cycles/degree; mean luminance, 192 cd/m²) (Fig. 2A). The grating could be

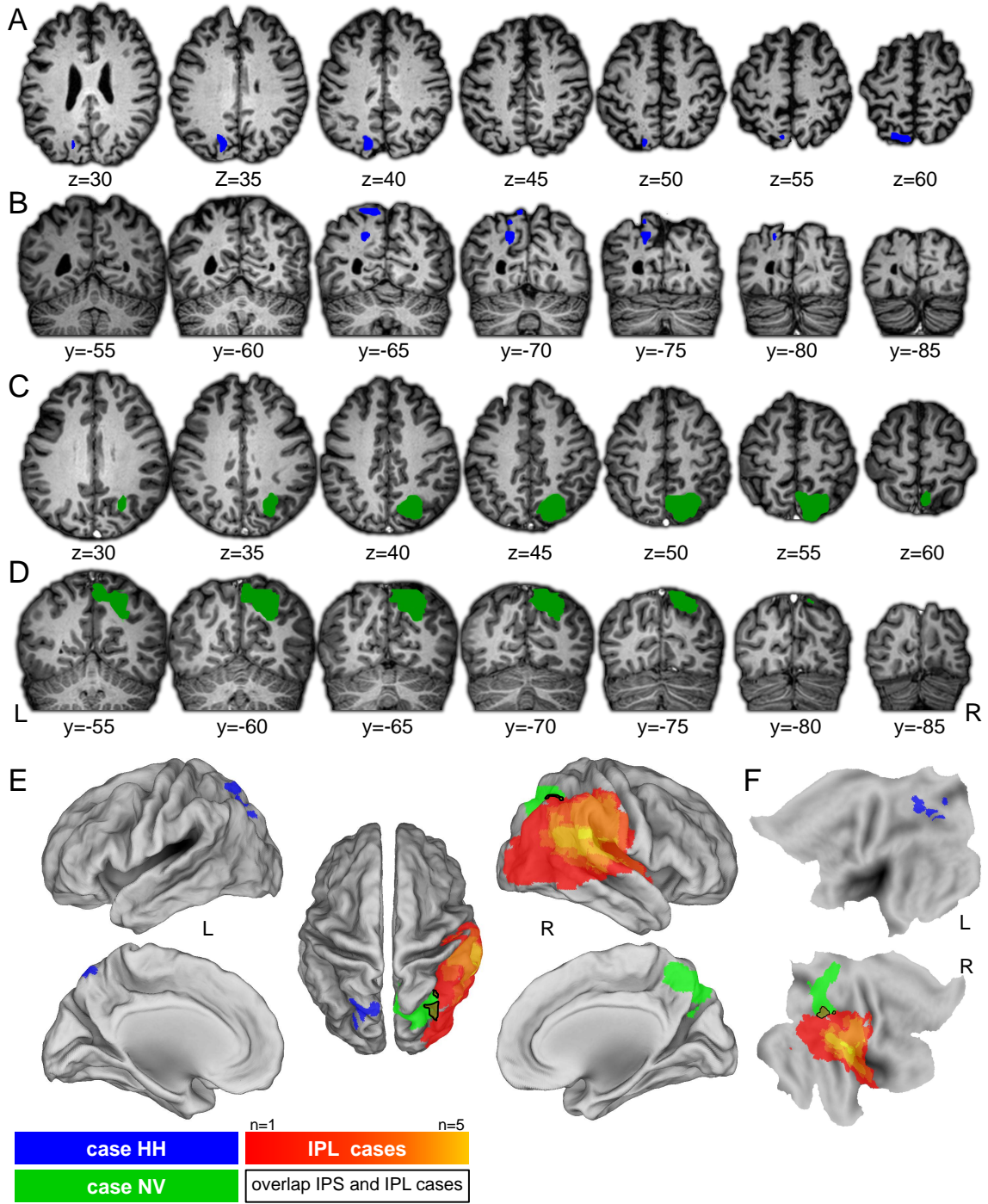


Figure 1 – Neuroanatomy of lesions. (A-D) Anatomy of the patients' brain on T1-weighted MR images, normalized to MNI space. The lesions of HH (A,B) and NV (day 4, C,D) are projected on axial (A,C) and coronal (B,D) slices. (E) Lesions in HH, NV and the 5 IPL cases projected onto a surface rendering of the brain (lateral, medial and dorsal view) (PALS Atlas, Caret 5.612 (Van Essen, 2005)). The black outline indicates the lesion overlap between case NV and one of the IPL cases (AN). (F) Projection of the lesions on the flattened brain surface.

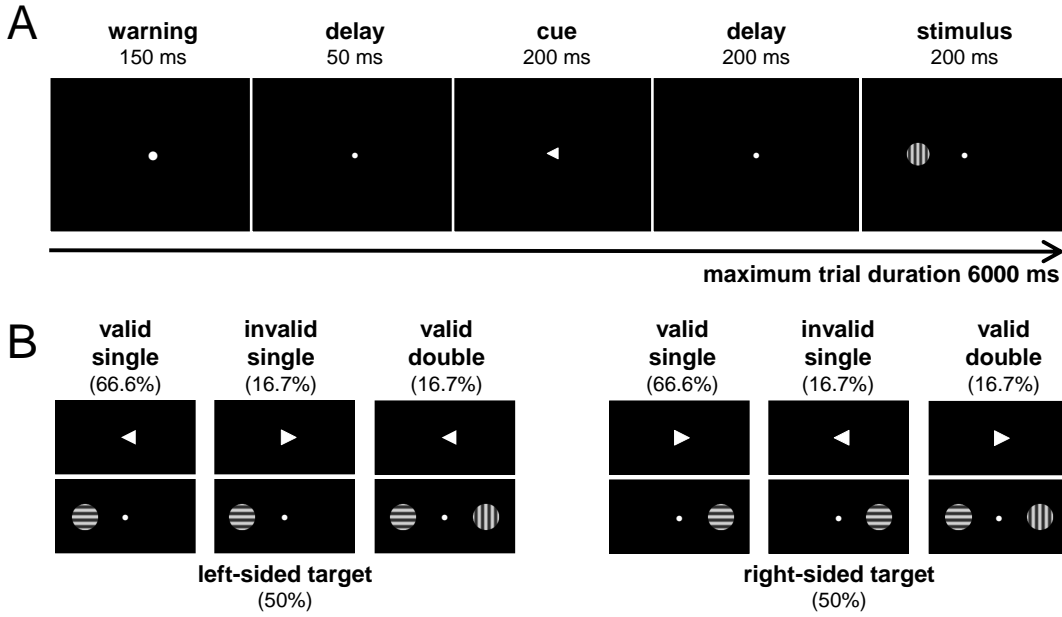


Figure 2 – Experimental paradigm (A) Example of the trial sequence. **(B)** The experimental design: target location (left-sided, right-sided) and trial type (valid/single, invalid/single, valid/double) as independent factors.

presented to the left or to the right at 7.6° eccentricity on the horizontal meridian. Its orientation was either horizontal (90°) or vertical (0°). With their right hand subjects held a response box with two response buttons. They were instructed to maintain fixation on the central fixation dot and select a button depending on the orientation of the target grating. In 66% of the trials (‘valid/single’) a single grating appeared at the cued location, in 17% of the trials (‘invalid/single’) a single grating appeared contralaterally to the cued location, and in 17% of the trials (‘valid/double’) the target grating appeared at the cued location together with a second, irrelevant grating at the contralateral location (Fig. 2B). The distracter orientation, horizontal or vertical, was pseudorandomly chosen with the constraint that each option occurred equally often and that it was congruent with the target orientation in half of trials and incongruent in the remaining half. The intertrial interval was paced by the subject’s response, with a minimum intertrial interval of 2250 ms. If no response was given, the trial was aborted after 6000 ms and the next trial was initiated. Subjects first received 24 training trials followed by 3 series of 120 trials separated by a brief pause. Gaze fixation was monitored by means of infrared eye monitoring (Viewpoint Eye Tracker; Arrington Research; Scottsdale, AZ) throughout the training and experimental runs.

As accuracy measure we used A' , a non-parametric estimate of how well the grating orientations can be discriminated (Snodgrass et al., 1985), with a value near 1.0 corresponding to good discriminability and a value near 0.5 corresponding to chance performance. We analyzed

the reaction times (RTs) of correct responses for each subject using an ex-Gaussian distribution probability-density model (Vossel et al., 2006; Lacouture and Cousineau, 2008). From the fitted function, we derived the mean (μ), standard deviation and exponential component in each subject.

The primary outcome analysis consisted of the contrast between invalid/single and valid/single ('invalidity effect') for contra- and ipsilesional targets and the contrast between valid/double and valid/single ('competition effect') for contra- and ipsilesional targets in HH and NV compared to age-matched controls. Inference was based on a modified t -test (Crawford and Garthwaite, 2002). As a second primary outcome measure we conducted a $3 \times 3 \times 2$ analysis of variance (ANOVA) with group (3 levels: IPS cases, IPL cases, healthy controls) as between-subjects factor and trial type (3 levels: valid/single, invalid/single, valid/double) and target location (2 levels: contralesional versus ipsilesional in patients, left-sided versus right-sided in healthy controls) as within-subjects factors. For NV, the behavioral data on day 4 were used. A non-parametric randomization test with 2000 iterations was used to determine the statistical significance of the obtained F -values: we repeatedly randomized the subject order, assigned the individual subjects to the levels of the factor 'group' according to the shuffled subject order, submitted the shuffled data to a $3 \times 3 \times 2$ ANOVA and saved the resulting F -values for each main and interaction effect. The F -values observed in the ANOVA on the original data were compared to distribution of F -values obtained using the randomization procedure. F -values in the right tail of the probability distribution (Bowman and Azzalini, 1997) ($P < 0.05$) were considered statistically significant (Fig. 3). Post-hoc analyses were conducted using the same randomization procedure: the 3 groups of subjects were compared in a pairwise manner ($2 \times 3 \times 2$ design) and correction for multiple contrasts was done using Bonferroni ($P < 0.05$).

Structural MRI

Structural and functional images were acquired on a 3 tesla Philips Intera system (Best, Netherlands) equipped with a head volume coil. Structural imaging sequences consisted of a T1-weighted 3D turbo-field-echo sequence (repetition time (TR) 9.6 ms, echo time (TE) 4.6 ms, in-plane resolution 0.97 mm, slice thickness 1.2 mm) and FLAIR image (TR 11000 ms, TE 150 ms, in-plane resolution 0.45 mm, slice thickness 4 mm). Using Statistical Parametric Mapping 2005 (SPM5) (Wellcome Trust Centre for Neuroimaging, London, UK, <http://www.fil.ion.ucl.ac.uk/spm>), we co-registered the T1 and FLAIR images of each patient. The boundary of the lesion was delineated on the individual MR images for every transverse slice (voxel-resolution $1 \times 1 \times 1$ mm³)

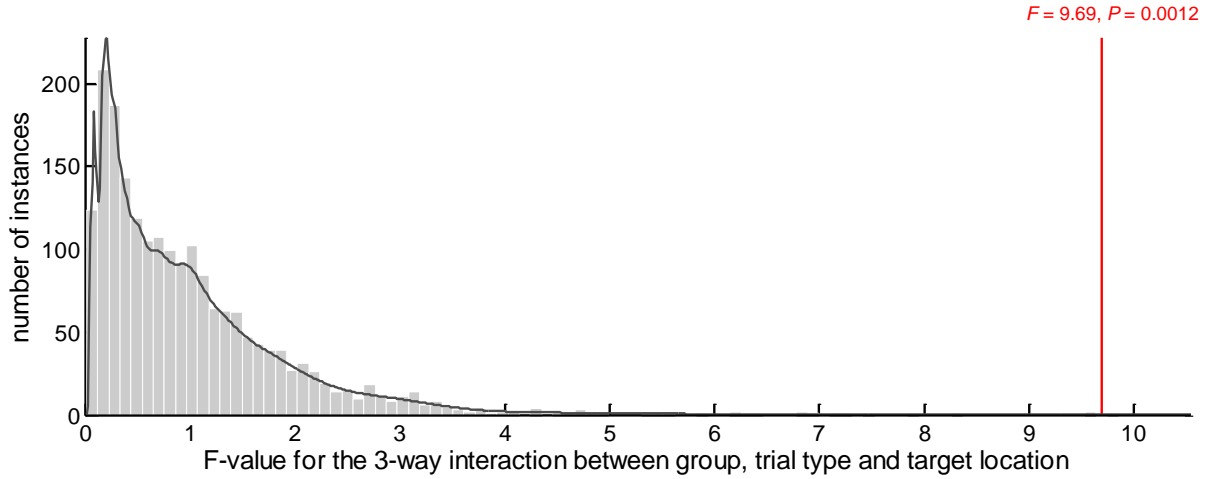


Figure 3 – Behavioral experiment The distribution of F -values corresponding to the 3-way interaction group \times trial type \times target location, was generated using a randomization procedure and is shown in grey. Its estimated density function is shown by the black curve. The F -value associated with the 3-way interaction in an ANOVA on the original data, is indicated by a red line.

with MRICron (Rorden et al., 2007) (www.cabiatl.com/mricro/mricron/index.html). The T1-weighted image was segmented and the resulting parameters were used to spatially normalize all images into the standard MNI space. A cost-function masking was used to prevent the damaged brain areas from biasing the transformation matrix. The spatial normalization involved both linear (12 parameters) and nonlinear ($7\times 9\times 7$ basis functions, 16 iterations) transformations (Ashburner and Friston, 1999). The match between each patient’s normalized brain and the template was carefully evaluated through visual inspection and use of a cross-hair yoked between the template and the normalized image.

Task-related fMRI experiment

In order to evaluate functional changes of parietal regions that were structurally intact in HH and NV, we acquired whole-brain functional scans consisting of T2* gradient-echo echoplanar images acquired continuously in ascending order (TR 2 s, TE 30 ms, 90° flip angle, 80×80 acquisition matrix, 2.75×2.75 mm² in-plane resolution, 36 3.75 mm thick axial slices without gap). NV underwent the fMRI experiment on day 107 when her lesion was reduced to a small portion of the SPL and her performance on the spatial cueing task had already normalized. Sixteen controls and the 2 IPS cases completed 6 runs with respectively 189 and 100 scans per run. Eye movements were registered in controls using an Applied Science Laboratory (Waltham, MA) infrared system and analyzed using an automatized procedure.

In controls the intertrial interval was fixed (2250 ms) and the orientation difference to be

discriminated relative to a 45° reference orientation was adjusted from run to run to reach an accuracy level of 75-85% across all conditions. The effects of trial type and target location on performance were tested with a repeated measures ANOVA. Each run consisted of 140 trials (60% valid/single, 20% invalid/single, 20% valid/double) and 28 null events. The stimuli and task were otherwise identical to what was used in the behavioral experiment. To ensure adequate task performance in the patients during fMRI (Price et al., 2006), they had to discriminate between a horizontal and vertical orientation, similarly to the behavioral experiment, and the intertrial interval was paced by their response with a minimum of 2000 ms and a maximum of 6000 ms.

The fMRI data were analyzed using SPM5. Following realignment, normalization and smoothing ($5 \times 5 \times 7$ mm³ Full Width Half Maximum, FWHM) we calculated for each subject the contrast image of invalid/single versus valid/single trials, as this contrast has been shown to activate IPL and TPJ (Corbetta et al., 2000; Vossel et al., 2006). We also calculated the contrast image of right-sided target versus left-sided target trials across all trial types, as well as the contrast image of right-sided versus left-sided target trials for the valid/double condition specifically. At a second level we determined whether the average contrast images were significantly different from zero (one-sample *t*-test: voxel-level threshold $P < 0.001$, cluster-level threshold $P < 0.05$ corrected for the entire brain volume (Poline et al., 1997)).

In order to evaluate whether task-related activity in structurally preserved parietal regions in the patients differed from that observed in healthy controls, we used a leave-one-out strategy: for each control we determined the effect size of the contrast of invalid/single minus valid/single trials in parietal volumes-of-interest (VOIs) which were defined on the basis of the same contrast in the remaining 15 controls. The effect size was defined as the weighted sum of β -values ($\beta_{\text{invalid left target}} + \beta_{\text{invalid right target}} - \beta_{\text{valid left target}} - \beta_{\text{valid right target}}$) and averaged across all voxels within a VOI. After having obtained a normal range of values, we determined the effect size in the patients in the VOIs defined in the controls. Inference was based on a modified *t*-test (Crawford and Garthwaite, 2002).

Resting-state fMRI experiment

We obtained resting-state fMRI in HH, NV (at day 107), and 62 controls. Two IPL cases (AN, PS) also participated as positive patient controls. During the resting-state fMRI run (425 s), we acquired 250 functional images with TR 1700 ms, TE 33 ms, 90° flip angle, 64×64 acquisition matrix, 3.59×3.59 mm² in-plane resolution, 32 axial slices with 4 mm thickness and no gap.

Subjects were instructed to remain awake with their eyes closed and not to think about anything in particular.

Following realignment, normalization and smoothing ($7 \times 7 \times 7$ mm³ FWHM) we defined the ventral and dorsal attention networks (Fox et al., 2006; Mantini et al., 2007) in the healthy control group by means of a template-matching procedure (Mantini et al., 2009). The resting-state networks (RSNs) were defined as Independent Component (IC) clusters (Esposito et al., 2005) with high across-subject consistency (proportion of subjects contributing to the cluster $> 66\%$) and a significant difference between intra- and extra-cluster correlations ($P < 0.001$, Bonferroni corrected for sample size) (Mantini et al., 2007). For each patient we derived the lesion fraction, the proportion of the lesion that spatially overlapped with each of the RSNs (threshold: $Z > 2$). We also examined in the patients how their lesion affected the topology of the ventral and dorsal attention networks (Fox et al., 2006). The similarity in topology between an IC in the individual subject and the RSNs in the group of controls (group RSNs) was estimated by measuring the spatial correlation between the maps, excluding the damaged brain area. We computed the spatial correlation between the ICs in each patient and the group RSNs and determined on that basis which ICs in each patient best matched the ventral and dorsal attention networks. Next, we compared the spatial correlation between the selected ICs in each patient and the group RSNs with the distribution of correlation values obtained in controls using the same procedure (leave-one out approach). Values in the left tail of the distribution ($P < 0.05$) were considered pathological.

As an additional measure of the functional integrity of TPJ, we analyzed the strength of its main inter- and intrahemispheric connections (Fox et al., 2006; Carter et al., 2010): we measured the resting-state functional connectivity (Carter et al., 2010) of right TPJ with left TPJ and right inferior frontal gyrus (IFG), respectively. The VOIs were defined by a sphere (6-mm radius) centered in the peak foci of the ventral attention network derived by ICA in controls (right TPJ: $x=56, y=-43, z=13$; left TPJ: $x=-59, y=-46, z=15$; right IFG: $x=58, y=10, z=9$). A representative time-course was obtained by averaging across all voxels within each VOI. Pearson's correlations were calculated for each subject using the VOI time-courses and converted to Z -scores by means of the Fisher's r -to- Z transformation (Carter et al., 2010). Statistical significance of the difference in Z -scores between patients and controls was assessed using a modified t -test (Crawford and Garthwaite, 2002).

Table 2 – Accuracy (A') in the behavioral and fMRI experiments L = left-sided target; R = right-sided target; A' = a non-parametric measure of performance. **(A)** Behavioral experiment: For HH and the IPL group values in **bold** indicate a significant performance decrease relative to the valid/single condition between the patient(s) and the elderly age-matched control group (n=17). For NV performance was compared with the young age-matched control group (n=14). **(B)** fMRI experiment: Values in **bold** indicate a significant performance decrease relative to valid/single condition between HH or NV and the healthy control group (n=16). s.d. = standard deviation.

case	valid/single		invalid/single		valid/double	
	L	R	L	R	L	R
A. Behavioral experiment:						
HH	0.97	0.96	0.95	0.83	0.88	0.50
NV, day 4	0.96	0.98	0.89	0.90	0.86	1.00
NV, day 107	0.99	1.00	1.00	0.98	0.98	0.98
IPL group	0.95	0.96	0.80	0.90	0.70	0.92
elderly healthy controls	0.97	0.98	0.95	0.95	0.91	0.88
young healthy controls	0.98	0.98	0.98	0.98	0.98	0.99
B. fMRI experiment:						
HH	0.99	0.99	0.96	0.78	0.97	0.77
NV	1.00	1.00	1.00	0.99	0.98	0.99
healthy controls	0.94	0.94	0.91	0.92	0.91	0.92
(s.d.)	(0.02)	(0.03)	(0.05)	(0.03)	(0.04)	(0.04)

Results

Behavioral experiment

According to on-line infrared eye tracking, patients and controls kept stable gaze fixation on the central fixation dot, except for one IPL case (AN) in whom eye fixation could not be monitored reliably. Analysis of the RTs did not yield any significant differences (Suppl. Table 2A).

HH performed the valid/single trials accurately, both for contra- ($t_{16}=-1.05$, $P=0.15$, (Crawford and Garthwaite, 2002)) and ipsilesional targets ($t_{16}=-0.50$, $P=0.31$; Fig. 4A, Table 2A). He however showed a pathological increase of the invalidity effect when invalid/single trials were compared to valid/single trials for contralesional targets ($t_{16}=1.75$, $P=0.049$). When valid/double trials were compared to valid/single trials for contralesional targets, A' dropped from 0.96 to 0.50, corresponding to chance performance (competition effect in HH compared to controls: $t_{16}=4.49$, $P=0.0002$). For ipsilesional targets, the invalidity effect ($t_{16}=0$, $P=0.50$) and the competition effect ($t_{16}=0.49$, $P=0.32$) did not differ from age-matched controls (Fig. 4A, Table 2A).

In NV, at day 4 performance during ipsilesional valid/single trials was within the normal range ($t_{13}=0.18$, $P=0.43$). Accuracy during contralesional valid/single trials however was decreased compared to age-matched controls ($t_{13}=1.80$, $P=0.047$; Fig. 4B, Table 2A). The in-

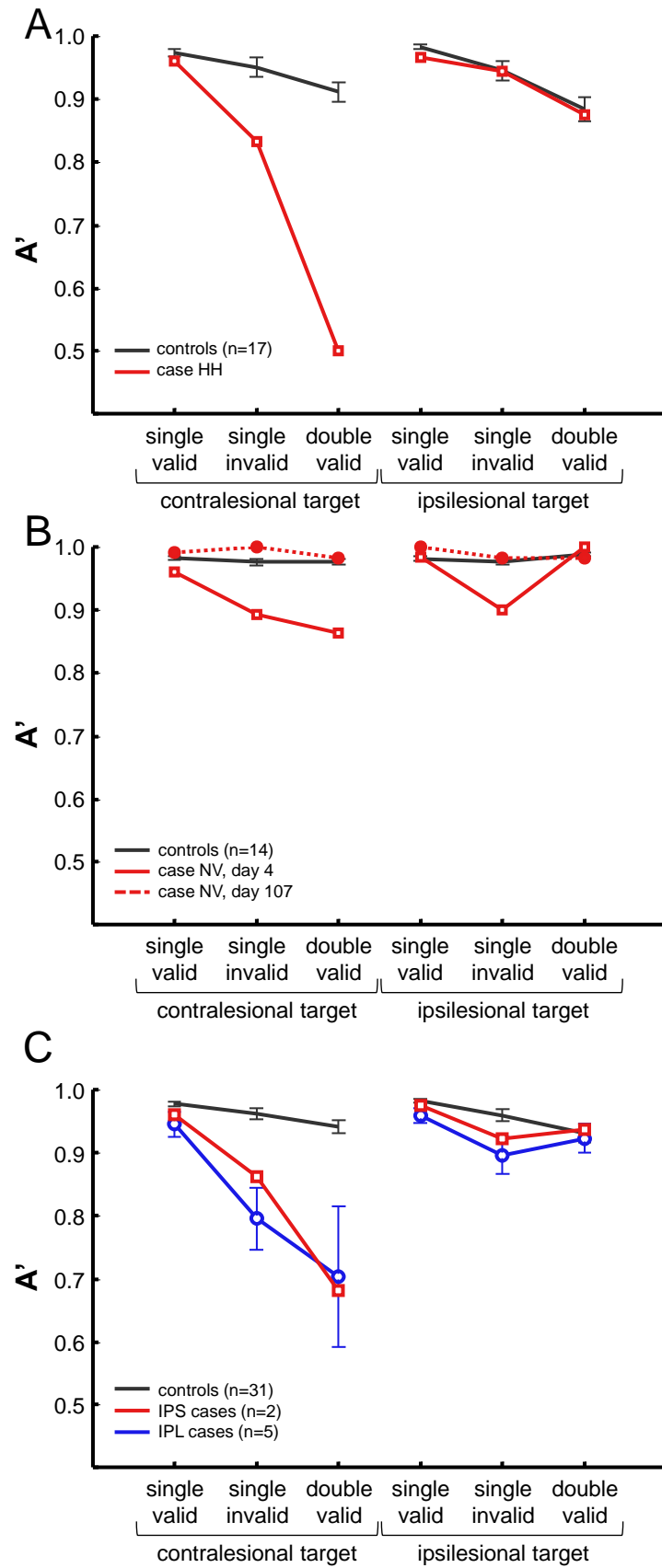


Figure 4 – Behavioral experiment: A' (A) HH (in red) versus age-matched controls (in black). (B) NV at day 4 (solid red line) and day 107 (dotted red line) versus age-matched controls (in black). (C) Group analysis. The mean values are plotted for the IPS group (HH, NV, red), the IPL group (in blue), and the control group. Error bars denote s.e.m.

validity effect (the reduction in A' from valid/single to invalid/single trials) was pathologically increased compared to controls, both for contra- ($t_{13}=2.90$, $P=0.006$) and for ipsilesional targets ($t_{13}=3.86$, $P=0.001$). This was also true when valid/double trials were compared to valid/single trials for contralesional targets ($t_{13}=4.35$, $P=0.0004$). For ipsilesional targets, the competition effect did not differ from healthy controls ($t_{13}=-0.48$, $P=0.32$). Three months later, when the lesion had regressed (Suppl. Fig. 1B), all outcome parameters in NV had normalized ($P>0.05$; Fig. 4B, Table 2A).

In 4 of the 5 IPL patients, the invalidity effect was increased for contralesional targets (Fig. 5A-D; AN: $t_{16}=1.70$, $P=0.05$; CK, $t_{16}=3.16$, $P=0.003$; MD: $t_{16}=2.92$, $P=0.006$; RE: $t_{16}=7.05$, $P<0.001$). In one patient (CK), it was also significantly increased for ipsilesional targets (Fig. 5B; $t_{16}=2.92$, $P=0.005$). In 3 of the IPL patients, the competition effect was significantly increased for contralesional targets (Fig. 5A, AN: $t_{16}=5.18$, $P<0.001$; Fig. 5C, MD: $t_{16}=5.35$, $P<0.001$; Fig. 5D, RE: $t_{16}=5.83$, $P<0.001$), with chance level performance in valid/double trials with contralesional targets. Performance of valid/double trials with ipsilesional targets was intact.

At the group level, a $3\times 3\times 2$ ANOVA with group (IPS, IPL, healthy controls), trial type (valid/single, invalid/single, valid/double) and target location (contra- versus ipsilesional for patients, left-sided versus right-sided attention for controls) as factors and A' as outcome measure revealed a three-way interaction ($F_{4,70}=9.69$, $P=0.001$; Fig. 4C, Fig. 3). We further evaluated this interaction effect by pairwise comparison between each of the groups.

When the IPS group was contrasted with controls, the three-way interaction between group, trial type and target location ($F_{2,62}=13.93$, $P=0.006$) and the two-way interactions between group and trial type ($F_{2,62}=4.59$, $P=0.03$) and between group and target location ($F_{1,31}=28.96$, $P=0.002$) were significant. In the IPS group the invalidity effect was larger than in controls for contralesional targets ($F_{1,31}=9.17$, $P=0.009$) but not for ipsilesional targets ($F_{1,31}=0.84$, $P=0.20$; Fig. 4C). The competition effect was also significantly larger than in controls for contralesional ($F_{1,31}=22.8$, $P=0.004$) but not for ipsilesional targets ($F_{1,31}=0.05$, $P=0.84$).

When the IPL group was contrasted with controls, the three-way interaction between group, trial type and target location ($F_{2,68}=13.16$, $P=0.001$) and the two-way interactions between group and trial type ($F_{2,68}=8.32$, $P=0.004$) and between group and target location ($F_{1,34}=20.36$, $P=0.0007$) were significant: The invalidity effect was larger in the IPL patients relative to controls for contralesional targets ($F_{1,34}=34.82$, $P<0.0001$; Fig. 4C), with a trend present for ipsilesional targets ($F_{1,34}=3.23$, $P=0.05$). The competition effect was significantly

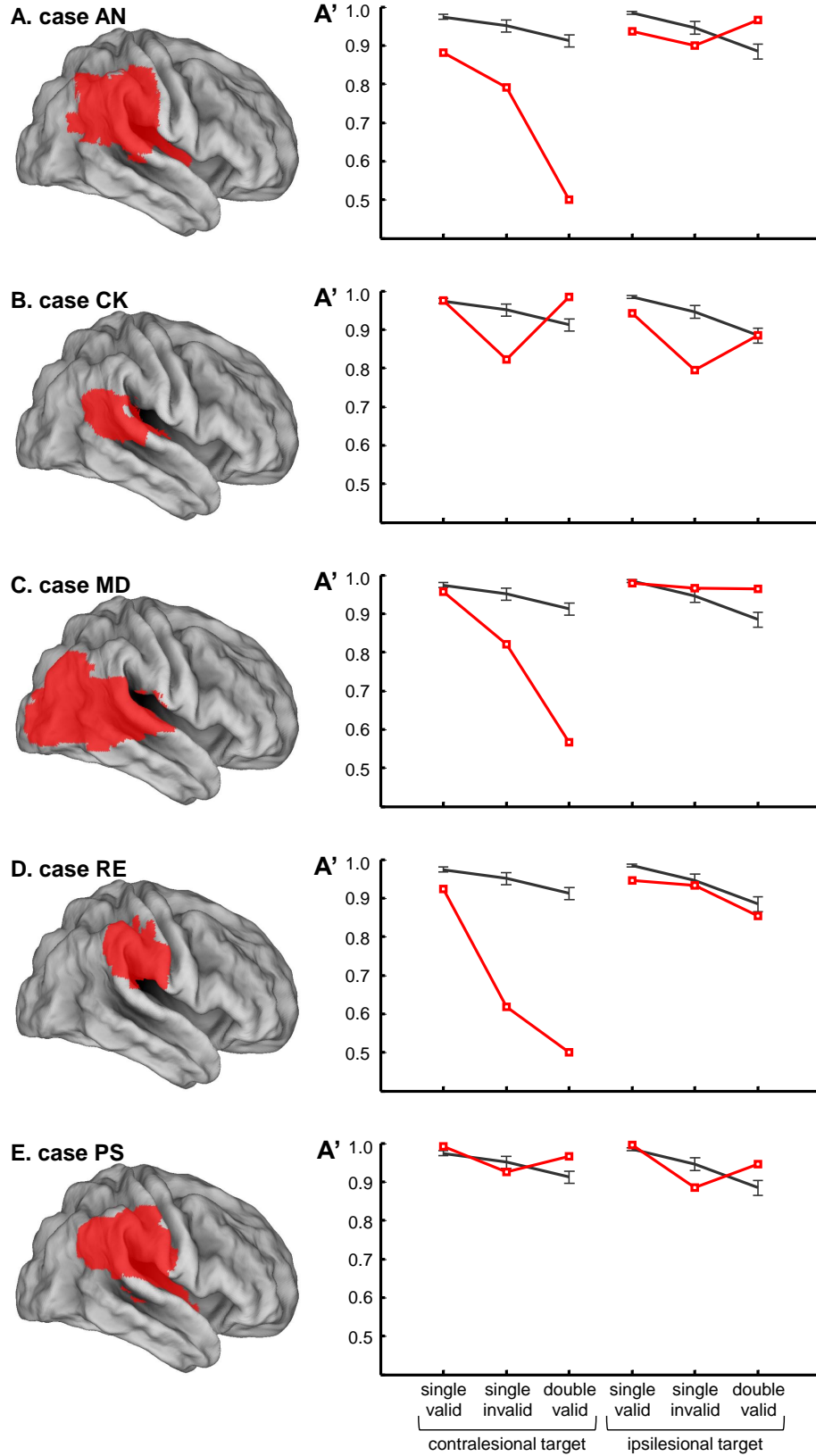


Figure 5 – Behavioral experiment: A' in the IPL group. **Left panel:** The lesions of the 5 IPL cases are projected onto a surface rendering of the brain (lateral view of the right hemisphere) (PALS Atlas, Caret 5.612; Van Essen et al., 2005). **Right panel:** Performance (A') of each IPL case (in *red*) versus age-matched elderly controls (in *black*). (A) Case AN. (B) Case CK. (C) Case MD. (D) Case RE. (E) Case PS.

larger relative to controls for contralesional ($F_{1,34}=23.13$, $P=0.0001$) but not for ipsilesional targets ($F_{1,34}=0.17$, $P=0.67$).

No significant differences were found between the IPS and IPL patient groups in the invalidity or competition effect, neither for contra- nor for ipsilesional targets (three-way interaction: $F_{2,10}=0.14$, $P=0.80$; Fig. 4C).

HH, AN, CK, MD and RE were re-tested 15 months later to evaluate the degree of recovery of their spatial attentional deficits (Suppl. Table 1A). The competition effect and the invalidity effect remained significantly increased in HH for contralesional targets ($t_{16}=4.17$, $P<.001$ and $t_{16}=2.33$, $P=0.02$, respectively). This was also true for the competition effect in AN ($t_{16}=5.18$, $P<.001$) and for the invalidity effect in MD ($t_{16}=1.76$, $P<0.05$).

Evaluation of functional integrity of IPL

HH, NV (day 107) and 16 healthy controls participated in an event-related fMRI study using the same paradigm as during the behavioral experiment. In controls the orientation difference to be discriminated during fMRI was 8.6° , averaged across subjects and runs (range $6-11^\circ$). We observed a significant main effect of trial type on A' ($F_{2,30}=6.34$, $P=0.005$; Table 2B) and mean RT ($F_{2,30}=10.96$, $P=0.0003$; Suppl. Table 2B). Eye movements did not differ between conditions (main effects of trial type and target location: $F_{2,30}=1.60$, $P=0.22$ and $F_{1,15}=0.71$, $P=0.41$, respectively). In HH, each run contained on average 91 trials with 59.7% valid/single trials, 20.2% invalid/single and 20.1% valid/double trials and in NV each run contained on average 90 trials with 60.3% valid/single trials, 19.8% invalid/single and 19.9% valid/double trials. Compared to controls, HH showed a pathological increase of the invalidity and competition effect for contralesional ($t_{15}=9.22$, $P<0.0001$ and $t_{15}=3.88$, $P=0.0007$, respectively) but not for ipsilesional targets ($P>0.40$), confirming the findings from the behavioral experiment (Table 2). NV's behavioral performance did not differ significantly from controls (Table 2), in agreement with her behavioral recovery.

In controls, the contrast between invalid/single minus valid/single trials activated left and right TPJ and IPL, left STG, left IPS and the medial wall of SPL, among other areas (Fig. 6A, Table 3). HH showed a normal activation pattern within these regions compared to controls (contrast invalid/single minus valid/single in HH versus controls $P>0.35$ in all regions; Fig. 6C; Table 3). The contrast of right-sided minus left-sided targets in controls activated the occipitoparietal cortex in the left hemisphere, including a posterior IPS focus corresponding to the lesion site in case HH ($x=-21$, $y=-78$, $z=33$, $Z=4.37$, $P=0.004$; Fig. 6B). In controls, activity

Table 3 – fMRI experiment: task-related fMRI activity Anatomical location and statistical assessment of parietal brain areas that showed significantly stronger activation in invalid/single relative to valid/single trials (voxel-level uncorrected $P < 0.001$, cluster-level corrected $P < 0.05$). Values in **bold** indicate a significant difference in the effect size of HH or NV and the healthy control group ($n=16$). *Legend:* STG, superior temporal gyrus; IPL, inferior parietal lobule; IPS, intraparietal sulcus; SPL, superior parietal lobule; TPJ, temporoparietal junction; MNI, Montreal Neurological Institute

region	MNI peak (x,y,z)	# voxels 27 mm ³	Z	mean effect size		
				controls (s.d.)	case HH	case NV
left STG	-63,-54,0	148	5.41	4.08 (1.90)	2.69	3.39
left IPL	-48,-48,33	164	4.59	4.33 (3.57)	5.82	7.25
left IPS	-33,-60,48	103	3.82	5.57 (4.00)	5.85	15.25
medial SPL	3,-63,51	209	4.48	6.85 (5.15)	6.62	5.58
right TPJ	57,-45,18	481	4.83	4.88 (2.84)	4.18	4.61

in this posterior IPS focus was higher for right-sided targets than left-sided targets even under double stimulation conditions ($t_{15}=2.35$, $P=0.03$; Fig. 6D), confirming the presence of an attentional effect within this visually responsive region (Yantis et al., 2002; Vandenberghe et al., 2005; Silver and Kastner, 2009; Bressler and Silver, 2010). In NV, the contrast invalid/single minus valid/single yielded significantly higher activity in left IPS compared to controls ($t_{15}=2.35$, $P=0.02$; Fig. 6C; Table 3).

HH, NV, 2 IPL cases and 62 controls also took part in a resting-state fMRI study. The structural lesion of patient HH exclusively mapped onto the dorsal attention network as defined in healthy controls (lesion fraction 58%; Fig. 7B). In NV (day 4), the principal overlap was also with the dorsal attention network (70% of her structural lesion; Fig. 7B) and, through its extension into SPL, with what is called the ventral attention network (which also includes an SPL component) (lesion fraction 6%; Fig. 7A) (Fox et al., 2006; Mantini et al., 2009). The main components however of the ventral attention network are IPL and specifically TPJ. The IPL patients’ lesion overlapped mainly with the ventral attentional network (lesion fraction 27%; Fig. 7A) and with the dorsal attentional network (lesion fraction 12%; Fig. 7B).

To evaluate functional changes of the RSNs in HH and NV, we assessed whether they could be identified in these patients and whether they corresponded in their topology to the RSNs in controls. Two IPL cases also participated as positive patient controls. The correspondence was estimated through spatial correlation across all voxels that were structurally intact in the individual patient. The correspondence between the ventral attention network in HH and NV and the ventral attention network in the group of controls ($r=0.39$ and $r=0.38$, respectively) lay well within the normal range of spatial correlations observed in healthy subjects (HH compared to controls: probability that a healthy control shows the same or a lower spatial correlation:

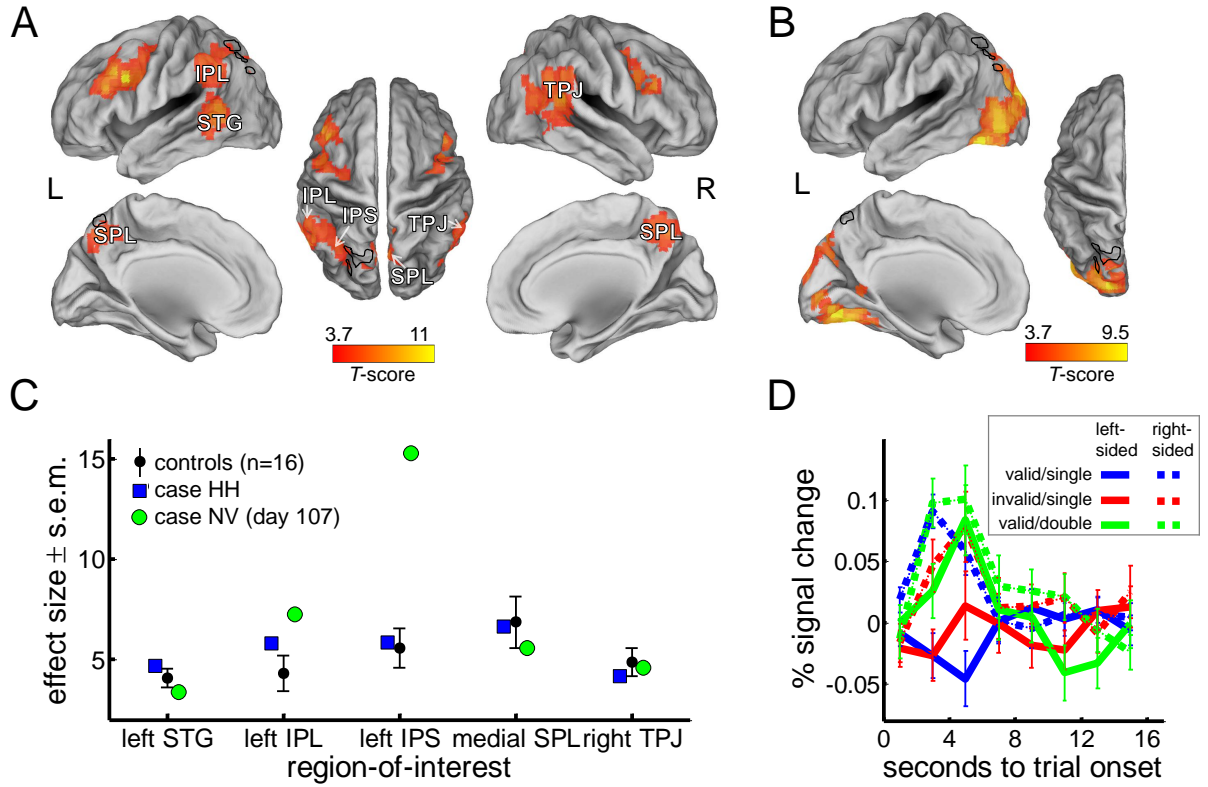


Figure 6 – Task-related fMRI (A) T -map, thresholded at voxel-level uncorrected $P < 0.001$, cluster-level FWE-corrected $P < 0.05$, obtained in 16 healthy controls corresponding to the contrast of invalid/single minus valid/single trials. (B) T -map obtained in healthy controls for the contrast of right-sided minus left-sided target trials. Anatomical location of HH's lesion is marked with a black outline. (C) Effect size, defined as the weighted sum of β -values, for case HH (in blue), case NV (in green) and controls (in black) in the left STG, IPL and IPS, the medial SPL and the right TPJ. Error bars represent s.e.m. across controls. (D) Time-activity curve in healthy controls. Average over 16 controls in the area of overlap (6 voxels) between the structural lesion of HH and the activity map shown in (D). Error bars represent s.e.m. across controls. *Legend:* blue: valid/single; red: invalid/single; green: valid/double; solid: left-sided target; dotted line: right-sided target.

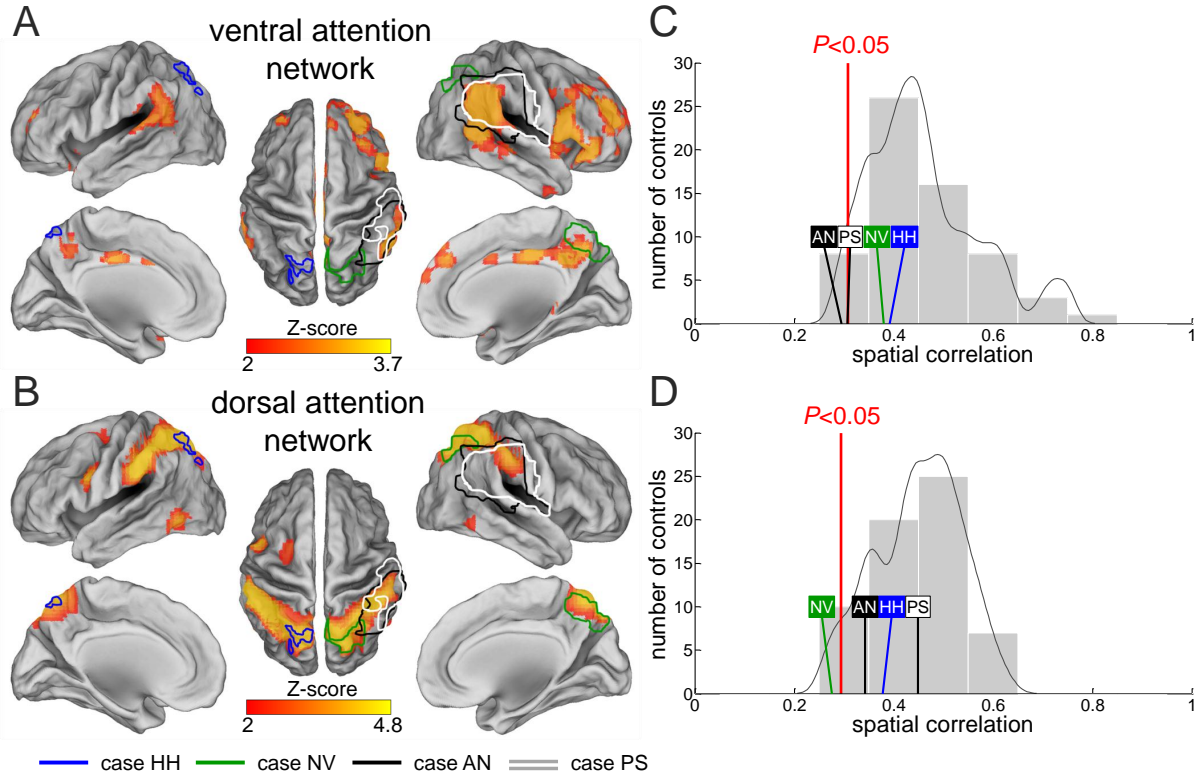


Figure 7 – Topology of RSNs in patients and healthy controls (A-B) The ventral and dorsal attention networks in 62 healthy controls are represented on fiducial cortical surfaces. The border of the lesions in HH (blue), NV (green) and 2 IPL cases (AN in black, PS in white) are superimposed on the surfaces. **(C-D)** For each of the RSNs, the spatial correlation of the best-matching IC in each patient with the group RSN, is compared to the distribution of correlations obtained in healthy controls using the same procedure. The distribution was described by estimating its density in a non-parametric way, shown by the black curve (Bowman and Azzalini, 1997). Pathological correlations are those in the lower 5% of the distribution. The relative threshold for pathology is indicated by a red line.

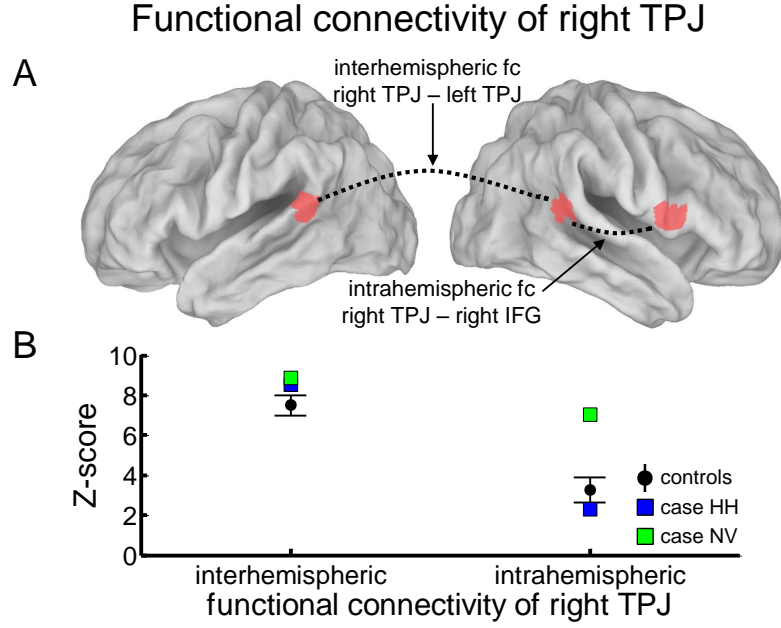


Figure 8 – Functional connectivity of right TPJ (A) Main functional connectivity within the ventral attention network, from right TPJ to left TPJ (interhemispheric) and to right IFG (intrahemispheric). (B) The strength of the connectivity, expressed in Z-scores, for HH (in *blue*) and NV (in *green*). Error bars represent s.e.m. across controls. Abbreviations: fc: functional connectivity.

$P=0.29$; NV compared to controls: $P=0.25$; Fig. 7C). In the IPL patients, it was significantly decreased (AN: $r=0.29$, $P=0.02$; PS: $r=0.31$, $P=0.04$). The topology of the dorsal attention network was preserved in HH and the IPL patients ($P>0.14$) but altered in NV ($r=0.28$, $P=0.03$; Fig. 7D). We also investigated by seed-based connectivity the strength of the main functional connections of TPJ in HH and NV (Fig. 8A)(Carter et al., 2010). Interhemispheric seed-based connectivity between left and right TPJ, and intrahemispheric connectivity between right TPJ and IFG were within the normal range for HH ($t_{61}=0.25$, $P=0.40$ and $t_{61}=-0.19$, $P=0.42$, respectively) and NV ($t_{61}=0.33$, $P=0.37$ and $t_{61}=0.77$, $P=0.22$, respectively; Fig. 8B).

Discussion

Isolated IPS lesions are extremely rare but can be highly informative as a critical test for how essential the role of IPS is in spatially selective attention. A long-standing discrepancy exists between functional imaging data in healthy controls and lesion mapping studies of spatial attention in this respect. The former highlight the contribution of superior parietal cortex to spatial attention (Corbetta et al., 1993; Nobre et al., 1997; Gitelman et al., 1999; Molenberghs et al., 2007, 2008; Mevorach et al., 2009), along with TPJ under specific circumstances (Corbetta et al., 2000; Downar et al., 2000; Vossel et al., 2009), while the latter almost invariably point to

IPL and TPJ as the critical parietal nodes (Vallar and Perani, 1986; Mort et al., 2003; Karnath et al., 2004). In the present study, isolated lesions of the posterior and the horizontal segment of the IPS (Fig. 1A-D) resulted in deficits of spatially selective attention (Fig. 4A,B). According to advanced functional imaging techniques (Fox et al., 2006; Mantini et al., 2009; Carter et al., 2010), the attentional deficits in HH could not be attributed to secondary functional effects occurring at a distance in IPL or TPJ (Fig. 6, 7, 8): The IPS lesion in HH did not alter the task-related activation in TPJ (Fig. 6C) nor the intra- and interhemispheric functional connectivity of TPJ (Carter et al., 2010) (Fig. 8B), and did not affect the topology of the ventral attention network (Fox et al., 2006) (Fig. 7C).

An unusually focal lesion in the posterior segment of the IPS (Fig. 1A,B) was sufficient to cause a significant behavioral deficit in spatial attention (Fig. 4A). The deficit occurred only when the need for spatially selective attention was high. HH performed within the normal range when a contralesional target on the cued location was presented without competing distracter (Table 2A,B). The high performance levels during valid/single trials rule out sensory factors as an explanation. The attentional deficit was strongly lateralized. The strict laterality of the deficit excludes non-spatial attentional processes, such as oddball detection, as an explanation.

At first sight the lateralization of the attentional deficit following a left-sided lesion differs from what one would predict based on the theory of right hemispheric dominance of visual attention (Weintraub and Mesulam, 1988). This theory accounts for the higher prevalence of clinical neglect following right-hemispheric lesions. HH had only mild signs of clinical neglect at initial testing. The right hemispheric dominance for spatial attention may possibly be less pronounced in the posterior part of IPS or may mainly hold for more severe degrees of clinical neglect (Mesulam, 2002). By and large, the contralateral retinotopic representations in IPS0-1 are symmetrical between left and right IPS (Silver et al., 2005) and more prominent than in more anterior parts of IPS (Silver et al., 2005; Swisher et al., 2007). The symmetrical representation in posterior IPS may therefore explain why HH's left-sided lesion provided a clearly lateralized spatial attention deficit.

In the intact brain this posterior IPS segment contains multiple retinotopically organized areas, including V7 (Tootell et al., 1998) or IPS0 (Silver et al., 2005) which forms a 'map cluster' with IPS1 sharing a common foveal representation (Swisher et al., 2007; Wandell et al., 2007; Silver and Kastner, 2009). These areas are sensitive to the direction of attention (Fig. 6D) (Yantis et al., 2002; Vandenberghe et al., 2005; Silver and Kastner, 2009; Bressler and Silver, 2010). Which exact retinotopic area HH's lesion mapped onto was not tested directly because of

the high demands to the patient of reliable retinotopic mapping in parietal cortex. It remains a topic for further investigation how the laterality of the spatial deficit is affected by the reference frame, retinotopic or nonretinotopic (Vandenberghe and Gillebert, 2009).

The main lesion in our second case, NV, at day 4 lay in the right IPS, but NV also had a concomitant smaller and strictly asymptomatic lesion in the left postcentral gyrus (Suppl. Fig. 1). It is most unlikely that this lesion contributed to the behavioral deficit in NV: her symptoms were strictly left lateralized, this region has not been implicated in attentional processing before and in fact, did not overlap with any of the activity maps obtained in the task-related fMRI experiment or with the RSNs. The right-hemispheric IPS lesion in NV co-localized with the area of overlap between VLSM maps in patients suffering from selective attention deficits and foci activated in healthy volunteers when subjects have to select between competing stimuli (Vandenberghe et al., 2005; Molenberghs et al., 2008). The increased competition effect for contralesional targets in NV is in line with transcranial magnetic stimulation studies, which showed that stimulation of the posterior parietal cortex can induce attentional deficits in healthy subjects in the visual field contralateral to the stimulation site under conditions of bilateral simultaneous stimulation (Pascual-Leone et al., 1994; Hung et al., 2005; Koch et al., 2005; Battelli et al., 2009). According to the MNI coordinates, the stimulation site used by Battelli et al. (2009) was centered within the middle segment of the IPS ($x=25$, $y=-64$, $z=51$) and corresponded to NV's lesion site. This IPS segment contains the putative homologue of area LIP, one of the key areas in the spatial attention network in monkeys (Gottlieb et al., 1998; Sereno et al., 2001; Vandenberghe and Gillebert, 2009).

NV's lesion extended into the SPL (Fig. 1C,D). Her attentional deficit therefore can be partly due to the role of SPL in spatial shifting (Vandenberghe et al., 2001; Yantis et al., 2002). The SPL extension in NV overlapped with one of the activity foci obtained when invalid versus valid cueing trials were contrasted in healthy volunteers (Fig. 6A). Unlike HH in whom the attentional deficit was strictly lateralized to contralesional targets, NV demonstrated a bilateral deficit in spatial shifting, as one would predict from the bilateral activation of SPL in shifting paradigms (Vandenberghe et al., 2001; Yantis et al., 2002; Molenberghs et al., 2007).

At day 107, the lesion had significantly diminished and this structural recovery was associated with a normalization of the behavioral parameters (Fig. 4B). We however still observed a relative hyperactivity in the contralesional IPS (Fig. 6C). Increased activity in the contralesional IPS therefore does not appear to be limited to the phase preceding neglect recovery (Corbetta et al., 2005; Corbetta, 2010) but may persist even when the attentional deficits have

fully recovered.

Our IPL cases were only mildly impaired on conventional tests for neglect. We included patients only with lesions restricted to parietal cortex and excluded patients with large middle cerebral artery infarctions (Verdon et al., 2010) or patients who were neurologically so impaired that they were unable to sit autonomously in front of a computer and perform a computerized test. Lesion overlap, lesion subtraction and VLSM studies revealing the role of IPL in neglect (Vallar and Perani, 1986; Mort et al., 2003; Karnath et al., 2004; Bays et al., 2010; Karnath et al., 2010) do not allow one to infer the prevalence of neglect following lesions restricted to IPL. In these studies, larger lesions extending beyond the area of overlap also contribute to the overlap.

The lesions of all our IPL cases were in the right hemisphere due to the concomitant language comprehension deficits associated with left IPL lesions. Our data do therefore not allow any conclusions about the role of the left IPL in attentional processing.

How does our experimental paradigm relate to the clinical syndromes of visual extinction and neglect? In the clinical test for visual extinction (Bender, 1952) subjects have to divide spatial attention and detect stimuli whereas in our study subjects had to orient attention based on a prior spatial cue and discriminate the orientation of a grating. In a previous (Molenberghs et al., 2008) and the current study (Suppl. Table 1), all patients with visual extinction had a deficit on our competition paradigm. A deficit on the competition paradigm, however, can occur without clinical visual extinction, at least in the chronic stage (Suppl. Table 1). Most probably, the competition paradigm is more sensitive than the clinical visual extinction test, as is the case for the invalidity paradigm compared to conventional clinical neglect tests (Table 1, Suppl. Table 1) (Posner et al., 1984; Egly et al., 1994; Friedrich et al., 1998). This higher sensitivity may be conferred by the standardized procedure and strict experimental control, short and fixed presentation duration and the large number of trials of each type presented in random order.

In contrast with Friedrich et al. (1998), our superior parietal patients showed clear attentional deficits during invalid spatial cueing trials and no quantitative difference compared to the IPL group (Fig. 4C). At the individual level, 3 of the IPL cases (Fig. 5A,C,D) showed a pattern of performance for contralesional targets that was highly similar to that of the IPS cases, both for the invalidity and the competition effect (Fig. 4A,B). Close inspection of the raw data that are available from the superior parietal group in the Friedrich et al. (1998) study in effect reveals an increase of the invalidity effect also in the superior parietal group. Furthermore, in that study the IPL group globally showed longer response times than the superior parietal group

during contralesional orienting even during single valid trials. A global difference in reaction times may have proportionally amplified the invalidity effect in the IPL group. In our study reaction times were matched between the IPL and the IPS group (Suppl. Table 2). Friedrich et al. (1998) focused on the comparison between contra- and ipsilesional orienting, while in one of our superior parietal cases, NV, the invalidity effect was increased in both directions. Such a bilateral effect would have escaped the type of analysis reported by Friedrich et al. (1998).

Previous imaging studies in healthy subjects and patients have led to functional-anatomical models where superior and inferior parietal regions fulfill different roles in spatially selective attention (Corbetta et al., 2008; Vandenberghe and Gillebert, 2009; Riddoch et al., 2010). The principal functional difference between the superior and the inferior parietal lesion patients in our study was the strict laterality of the deficit following lesions of the posterior segment of IPS (Fig. 4A) compared to more anterior IPS (Fig. 4B) and TPJ lesions where in some cases the invalidity effect tended to be increased also for ipsilesional targets (Fig. 4C, 5).

For the first time we provide lesion-based evidence that lesions of this posterior IPS segment can cause lateralized spatial-attentional deficits. Our data show that right-sided IPL lesions are not necessary to create a lateralized attentional defect following parietal damage, in contrast to what previous models of spatial attention would predict (Corbetta and Shulman, 2002). Of course, different experimental paradigms may reveal functional dissociations between IPS and IPL cases and the laterality of spatial attentional deficits following left-sided lesions may differ depending on the location of the IPS lesion along the anterior-posterior axis. This is a subject for future investigation. At present, this detailed study of the consequences of superior parietal lesions provides unequivocal evidence that the superior parietal cortex critically contributes to spatial orienting of attention independently of IPL/TPJ.

Acknowledgments

We thank Natalie Nelissen, Guy Orban and Mathieu Vandenbulcke for helpful comments on an earlier version of this paper. We are most grateful to the patients who participated in this research. Supported by Research Foundation Flanders (FWO), Flanders, Belgium (G0668.07 ESF EuroCores Program), Katholieke Universiteit Leuven (OT/08/56) and Federaal Wetenschapsbeleid belspo (Inter-University Attraction Pole P6/29). CRG is a PhD research fellow, DM a postdoctoral research fellow and RV a senior clinical investigator of the FWO.

References

- Alstott J, Breakspear M, Hagmann P, Cammoun L, Sporns O, Modeling the impact of lesions in the human brain. *PLoS Comput Biol* 2009; 5: 1–12.
- Ashburner J, Friston K, Nonlinear spatial normalization using basis functions. *Hum Brain Mapp* 1999; 7: 254–266.
- Battelli L, Alvarez GA, Carlson T, Pascual-Leone A, The role of the parietal lobe in visual extinction studied with transcranial magnetic stimulation. *J Cogn Neurosci* 2009; 21: 1946–1955.
- Bays PM, Singh-Curry V, Gorgoraptis N, Driver J, Husain M, Integration of goal- and stimulus-related visual signals revealed by damage to human parietal cortex. *J Neurosci* 2010; 30: 5968–5978.
- Bender M. Disorders in perception: With particular reference to the phenomena of extinction and displacement. Springfield, IL: C.C. Thomas; 1952.
- Bowman A, Azzalini A. Applied smoothing techniques for data analysis. New York: Oxford University Press; 1997.
- Bressler DW, Silver MA, Spatial attention improves reliability of fmri retinotopic mapping signals in occipital and parietal cortex. *Neuroimage* 2010; 53: 526–533.
- Bundesen C, Habekost T, Kyllingsbaek S, A neural theory of visual attention: Bridging cognition and neurophysiology. *Psychol Rev* 2005; 112: 291–328.
- Carter AR, Astafiev SV, Lang CE, Connor LT, Rengachary J, Strube MJ, et al., Resting interhemispheric functional magnetic resonance imaging connectivity predicts performance after stroke. *Ann Neurol* 2010; 67: 365–375.
- Corbetta M, Functional connectivity and neurological recovery. *Dev Psychobiol*. In press 2010.
- Corbetta M, Kincade JM, Ollinger JM, McAvoy MP, Shulman GL, Voluntary orienting is dissociated from target detection in human posterior parietal cortex. *Nat Neurosci* 2000; 3: 292–297.
- Corbetta M, Kincade MJ, Lewis CL, Snyder AZ, Sapir A, Neural basis and recovery of spatial attention deficits in spatial neglect. *Nat Neurosci* 2005; 8: 1603–1610.

- Corbetta M, Miezin F, Shulman G, Petersen S, A PET study of visuospatial attention. *J Neurosci* 1993; 13: 1202–1226.
- Corbetta M, Patel G, Shulman GL, The reorienting system of the human brain: from environment to theory of mind. *Neuron* 2008; 58: 306–324.
- Corbetta M, Shulman G, Control of goal-directed and stimulus-driven attention in the brain. *Nat Rev Neurosci* 2002; 3: 201–215.
- Crawford JR, Garthwaite PH, Investigation of the single case in neuropsychology: confidence limits on the abnormality of test scores and test score differences. *Neuropsychologia* 2002; 40: 1196–1208.
- Critchley M, *The Parietal Lobes*. London: Edward Arnold; 1953.
- Downar J, Crawley AP, Mikulis DJ, Davis KD, A multimodal cortical network for the detection of changes in the sensory environment. *Nat Neurosci* 2000; 3: 277–283.
- Driver J, Blankenburg F, Bestmann S, Ruff CC, New approaches to the study of human brain networks underlying spatial attention and related processes. *Exp Brain Res* 2010; 206: 153–162.
- Egley R, Driver J, Rafal RD, Shifting visual attention between objects and locations: evidence from normal and parietal lesion subjects. *J Exp Psychol Gen* 1994; 123: 161–177.
- Esposito F, Scarabino T, Hyvarinen A, Himberg J, Formisano E, Comani S, et al., Independent component analysis of fMRI group studies by self-organizing clustering. *Neuroimage* 2005; 25: 193–205.
- Fox MD, Corbetta M, Snyder AZ, Vincent JL, Raichle ME, Spontaneous neuronal activity distinguishes human dorsal and ventral attention systems. *Proc Natl Acad Sci USA* 2006; 103: 10046–10051.
- Friedrich FJ, Egley R, Rafal RD, Beck D, Spatial attention deficits in humans: a comparison of superior parietal and temporal-parietal junction lesions. *Neuropsychology* 1998; 12: 193–207.
- Gitelman DR, Nobre AC, Parrish TB, LaBar KS, Kim YH, Meyer JR, et al., A large-scale distributed network for covert spatial attention: further anatomical delineation based on stringent behavioural and cognitive controls. *Brain* 1999; 122: 1093–1106.

- Gottlieb JP, Kusunoki M, Goldberg ME, The representation of visual salience in monkey parietal cortex. *Nature* 1998; 391: 481–483.
- Grandjean D, Sander D, Lucas N, Scherer KR, Vuilleumier P, Effects of emotional prosody on auditory extinction for voices in patients with spatial neglect. *Neuropsychologia* 2008; 46: 487–496.
- He BJ, Shulman GL, Snyder AZ, Corbetta M, The role of impaired neuronal communication in neurological disorders. *Curr Opin Neurol* 2007; 20: 655–660.
- Hung J, Driver J, Walsh V, Visual selection and posterior parietal cortex: Effects of repetitive transcranial magnetic stimulation on partial report analyzed by Bundesen’s Theory of Visual Attention. *J Neurosci* 2005; 25: 9602–9612.
- Husain M, Nachev P, Space and the parietal cortex. *Trends Cogn Sci* 2007; 11: 30–36.
- Karnath HO, Berger MF, Kker W, Rorden C, The anatomy of spatial neglect based on voxelwise statistical analysis: a study of 140 patients. *Cereb Cortex* 2004; 14: 1164–1172.
- Karnath HO, Ferber S, Himmelbach M, Spatial awareness is a function of the temporal not the posterior parietal lobe. *Nature* 2001; 411: 950–953.
- Karnath HO, Himmelbach M, Kker W, The cortical substrate of visual extinction. *Neuroreport* 2003; 14: 437–442.
- Karnath HO, Rennig J, Johannsen L, Rorden C, The anatomy underlying acute versus chronic spatial neglect: a longitudinal study. *Brain*. In press 2010.
- Koch G, Oliveri M, Torriero S, Caltagirone C, Modulation of excitatory and inhibitory circuits for visual awareness in the human right parietal cortex. *Exp Brain Res* 2005; 160: 510–516.
- Koyama M, Hasegawa I, Osada T, Adachi Y, Nakahara K, Miyashita Y, Functional magnetic resonancy imaging of Macaque monkeys performing visually guided saccade tasks: Comparison of cortical eye fields with humans. *Neuron* 2004; 41: 795–807.
- Lacouture Y, Cousineau D, How to use matlab to fit the ex-gaussian and other probability functions to a distribution of response times. *Tutorials in quantitative methods for psychology* 2008; 4: 35–45.

- Mantini D, Corbetta M, Perrucci MG, Romani GL, Gratta CD, Large-scale brain networks account for sustained and transient activity during target detection. *Neuroimage* 2009; 44: 265–274.
- Mantini D, Perrucci MG, Gratta CD, Romani GL, Corbetta M, Electrophysiological signatures of resting state networks in the human brain. *Proc Natl Acad Sci USA* 2007; 104: 13170–13175.
- Mesulam M, Attentional networks, confusional states and neglect syndromes. In: Mesulam M, editor. *Principles of behavioral and cognitive neurology*. New York NY: Oxford University Press; 2000. p 174–256.
- Mesulam M, Functional anatomy of attention and neglect: from neurons to networks. In: Karnath HO, Milner D, Valler G, editors. *The cognitive and neural bases of spatial neglect*. Oxford: Oxford University Press; 2002. p 33–45.
- Mesulam MM, Large-scale neurocognitive networks and distributed processing for attention, language, and memory. *Ann Neurol* 1990; 28: 597–613.
- Mevorach C, Shalev L, Allen HA, Humphreys GW, The left intraparietal sulcus modulates the selection of low salient stimuli. *J Cogn Neurosci* 2009; 21: 303–315.
- Molenberghs P, Gillebert CR, Peeters R, Vandenberghe R, Convergence between lesion-symptom mapping and functional magnetic resonance imaging of spatially selective attention in the intact brain. *J Neurosci* 2008; 28: 3359–3373.
- Molenberghs P, Mesulam MM, Peeters R, Vandenberghe R, Re-mapping attentional priorities: Differential contribution of superior parietal lobule and intraparietal sulcus. *Cereb Cortex* 2007; 17: 2703–2712.
- Mort DJ, Malhotra P, Mannan SK, Rorden C, Pambakian A, Kennard C, et al., The anatomy of visual neglect. *Brain* 2003; 126: 1986–1997.
- Nobre AC, Sebestyen GN, Gitelman DR, Mesulam MM, Frackowiak RS, Frith CD, Functional localization of the system for visuospatial attention using positron emission tomography. *Brain* 1997; 120: 515–533.
- Orban GA, Claeys K, Nelissen K, Smans R, Sunaert S, Todd JT, et al., Mapping the parietal cortex of human and non-human primates. *Neuropsychologia* 2006; 44: 2647–2667.

- Pascual-Leone A, Gomez-Tortosa E, Grafman J, Alway D, Nichelli P, Hallett M, Induction of visual extinction by rapid-rate transcranial magnetic stimulation of parietal lobe. *Neurology* 1994; 44: 494–498.
- Poline JB, Worsley KJ, Evans AC, Friston KJ, Combining spatial extent and peak intensity to test for activations in functional imaging. *Neuroimage* 1997; 5: 83–96.
- Posner MI, Walker JA, Friedrich FJ, Rafal RD, Effects of parietal injury on covert orienting of attention. *J Neurosci* 1984; 4: 1863–1874.
- Price CJ, Crinion J, Friston KJ, Design and analysis of fMRI studies with neurologically impaired patients. *J Magn Reson Imaging* 2006; 23: 816–826.
- Riddoch MJ, Chechklacz C, Mevorach C, Mavritsaki E, Allen H, Humphreys GW, The neural mechanisms of visual selection: the view from neuropsychology. *Ann NY Acad Sci* 2010; 1191: 156–181.
- Rorden C, Karnath HO, Bonilha L, Improving lesion-symptom mapping. *J Cogn Neurosci* 2007; 19: 1081–1088.
- Sack AT, Using non-invasive brain interference as a tool for mimicking spatial neglect in healthy volunteers. *Restor Neurol Neurosci* 2010; 28: 485–497.
- Sereno MI, Pitzalis S, Martinez A, Mapping of contralateral space in retinotopic coordinates by a parietal cortical area in humans. *Science* 2001; 294: 1350–1354.
- Sheremata SL, Bettencourt KC, Somers DC, Hemispheric asymmetry in visuotopic posterior parietal cortex emerges with visual short-term memory load. *J Neurosci* 2010; 30: 12581–12588.
- Silver MA, Kastner S, Topographic maps in human frontal and parietal cortex. *Trends Cogn Sci* 2009; 13: 488–495.
- Silver MA, Ress D, Heeger DJ, Topographic maps of visual spatial attention in human parietal cortex. *J Neurophysiol* 2005; 94: 1358–1371.
- Snodgrass J, Levy-Berger G, Haydon M, *Human Experimental Psychology*. New York: Oxford University Press; 1985.

- Swisher JD, Halko MA, Merabet LB, McMains SA, Somers DC, Visual topography of human intraparietal sulcus. *J Neurosci* 2007; 27: 5326–5337.
- Ticini LF, de Haan B, Klose U, Ngele T, Karnath HO, The role of temporo-parietal cortex in subcortical visual extinction. *J Cogn Neurosci* 2010; 22: 2141–2150.
- Tootell RB, Hadjikhani N, Hall EK, Marrett S, Vanduffel W, Vaughan JT, et al., The retinotopy of visual spatial attention. *Neuron* 1998; 21: 1409–1422.
- Vallar G, Perani D, The anatomy of unilateral neglect after right hemisphere stroke lesions: A clinical CT scan correlation study in man. *Neuropsychologia* 1986; 24: 609–622.
- Van Essen DC, A population-average, landmark- and surface-based (PALS) atlas of human cerebral cortex. *Neuroimage* 2005; 28: 635–662.
- Vandenberghe R, Geeraerts S, Molenberghs P, Lafosse C, Vandebulcke M, Peeters K, et al., Attentional responses to unattended stimuli in human parietal cortex. *Brain* 2005; 128: 2843–2857.
- Vandenberghe R, Gillebert CR, Parcellation of human parietal cortex: converging evidence from functional imaging in the intact human brain and patient lesion studies (invited review). *Behav Brain Res* 2009; 199: 171–182.
- Vandenberghe R, Gitelman DR, Parrish TB, Mesulam MM, Functional specificity of superior parietal mediation of spatial shifting. *Neuroimage* 2001; 14: 661–673.
- Verdon V, Schwartz S, Lovblad KO, Hauert CA, Vuilleumier P, Neuroanatomy of hemispatial neglect and its functional components: a study using voxel-based lesion-symptom mapping. *Brain* 2010; 133: 880–894.
- Vossel S, Thiel CM, Fink GR, Cue validity modulates the neural correlates of covert endogenous orienting of attention in parietal and frontal cortex. *Neuroimage* 2006; 32: 1257–1264.
- Vossel S, Weidner R, Thiel CM, Fink GR, What is "odd" in Posner's location-cueing paradigm? Neural responses to unexpected location and feature changes compared. *J Cogn Neurosci* 2009; 21: 30–41.
- Wandell BA, Dumoulin SO, Brewer AA, Visual field maps in human cortex. *Neuron* 2007; 56: 366–383.

- Weintraub S, Mesulam MM, Visual hemispatial inattention: stimulus parameters and exploratory strategies. *J Neurol Neurosurg Psychiatry* 1988; 51: 1481–1488.
- Yantis S, Schwarzbach J, Serences JT, Carlson RL, Steinmetz MA, Pekar J, et al., Transient neural activity in human parietal cortex during spatial attention shifts. *Nat Neurosci* 2002; 5: 995–1003.